DNA Binding, Solubility, and Partitioning Characteristics of Extended Lexitropsins

Robert V. Fishleigh,[†] Keith R. Fox,[‡] Abedawn I. Khalaf,[§,||] Andrew R. Pitt,[§] Martin Scobie,[§,||] Colin J. Suckling,[§] John Urwin,[§,||] Roger D. Waigh,*[,||] and Stephen C. Young[†]

Proteus Molecular Design Ltd., Proteus House, Lyme Green Business Park, Macclesfield, Cheshire SK11 0JL, England, Department of Physiology and Pharmacology, University of Southampton, Bassett Crescent East, Southampton SO16 7PX, England, Department of Pure and Applied Chemistry, University of Strathclyde, Glasgow G1 1XL, Scotland, and Department of Pharmaceutical Sciences, Strathclyde Institute for Biomedical Sciences, 27 Taylor Street, Glasgow G4 0NR, Scotland

Received December 20, 1999

Four new ligands that bind to the minor groove of DNA have been designed, synthesized, and evaluated by DNA footprinting. Two of the ligands are polyamides containing central regions with five or six *N*-methylpyrrole units, conferring hydrophobicity and good binding affinity but without retaining the correct spacing for hydrogen bonding in the base of the minor groove. The two remaining ligands have central regions which are head-to-head-linked polyamides, in which the linker is designed to improve the phasing of hydrogen bonding of the ligand with the floor of the minor groove. The highest affinity was obtained with the two polypyrroles without headgroup spacers, indicating that H-bond phasing is secondary in determining affinity compared to the major hydrophobic driving force. With a dimethylaminoalkyl group, representing a moiety with modest base strength, at both ends, water solubility is good and pH-partition theory predicts that penetration through lipid membranes will be enhanced, compared to strongly basic amidine analogues of the alkaloid precursors. All four compounds bind to DNA, with strong selectivity for AT sequences but some tolerance of GC base pairs and subtle individual preferences. The data show that very high affinities can be anticipated for future compounds in this series, but drug design must take account of overall physicochemical properties as well as the details of hydrogen bonding between ligands and the floor of the minor groove.

Introduction

The attractions of drug design where the ligand is directed at the primary coding sequences of DNA are many. Such a ligand, should it be sufficiently sequence-selective, would offer the prospect of gene control in diseases where genetic malfunction is the primary cause, such as cancer. In addition, there are exciting possibilities for the treatment of parasitic diseases, where the DNA possesses sequences which do not occur in the host.

Sequence selectivity is not a major feature of the early type of intercalating ligands, such as ethidium, but much attention has been devoted in recent years to the development of 'lexitropsins', which bind to the minor groove of DNA and thus have a greater chance of reading the information which is provided by the base-pair sequence as part of the usual process of transcription. It was found quite early in these studies that the natural polypyrroles, such as netropsin **(1)** and distamycin **(2)**, showed almost total selectivity for AT rather than GC sequences.[1] Very recently, it has been shown that these compounds show a degree of selectivity for some specific AT sequences over others.[2,3]

An important advance was made in ligand design[4] when the *N*-methylpyrrole units of the natural products were replaced with other five-membered heterocyclic rings, in particular imidazole, which changed the sequence-binding preference from AT to GC. A combination of these units offers the possibility of designing molecules to bind preferentially to any given double-stranded DNA sequence. Additionally, it is necessary to extend the length of the molecule to read considerably more than the four base pairs which bind the natural products, if a useful level of selectivity is to be achieved,[5] which may require the use, for example, of bifunctional linkers[6] to join chains of amide-bonded heterocycles. A significant variation on this approach allows the chain to double back on itself.[7] Such a 'hairpin' structure fills the minor groove and reads the sequence information more efficiently than a single chain but requires the construction of a considerably larger molecule, up to double the length of the sequence which is being read.

The central part of the ligand must be hydrophobic, since the main driving force for binding is the expulsion of water from the minor groove, itself a largely hydrophobic environment with a capacity for hydrogen bonding at the bottom of the groove. A recent thermodynamic study[8] has shown that binding in the minor groove of a DNA dodecamer by Hoechst 33258 is dominated by hydrophobic forces; clearly, new ligands must have large nonpolar regions if they are to show high affinity. A major concern in drug design, therefore, is the water

* To whom correspondence should be addressed. Tel: 0141-548-4355. Fax: 0141-552-6443. E-mail: r.d.waigh@strath.ac.uk.
[†] Proteus Molecular Design Ltd.
[‡] University of Southampton.
[§] University of Strathclyde.
[||] Strathclyde Institute for Biomedical Sciences.

10.1021/jm990620e CCC: $19.00
Published on Web 08/03/2000

solubility of a ligand composed largely of nonpolar subunits and, if this is overcome by the use of more than one basic end group, the effect that this will have on the ability of the molecule to penetrate lipid membranes by passive diffusion.

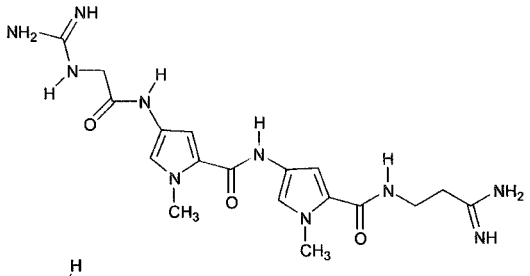

1

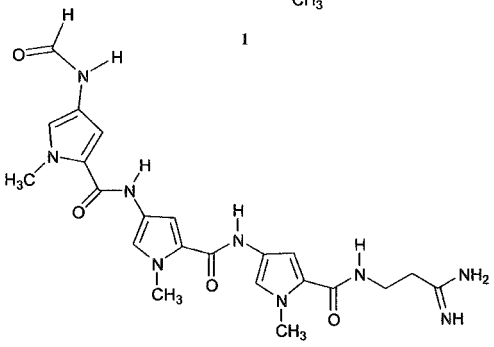

2

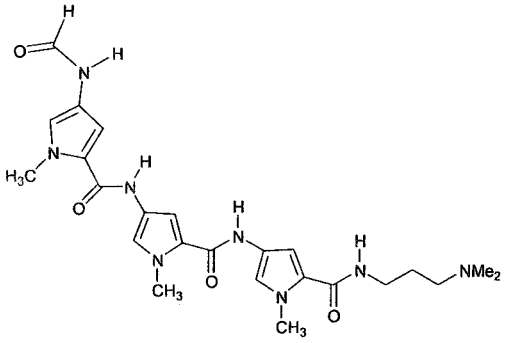

3

To test these concepts, we have synthesized four new ligands **4**−**7**, which combine building blocks known to give good DNA binding, and have correlated their DNA binding with their calculated partitioning properties. Ligands **4** and **5** are extended polyamides, with long chains of nonpolar *N*-methylpyrroles rendered more soluble by dimethylamino groups at both ends. Ligands **6** and **7** are both head-to-head-linked polypyrroles, with a linker which has been designed to improve H-bonding in the base of the minor groove: in both cases the linker is more hydrophilic than the polypyrrole chains. The dimethylamino end groups of structures **4**−**7** were chosen for three reasons. First, they have been used before[9] and have been shown to be consistent with good DNA binding. Second, the synthetic methods for their incorporation are well-established, and third, we wished to use tertiary bases, which would have lower pK_a values than amidines, guanidines, or secondary bases. This is highly significant when pH-partition theory is applied to these molecules.

The application of pH-partition theory to drugs with a lipophilic structure and one basic group is well-established;[10] it is a combination of the Henderson−

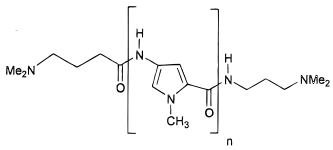

4 n = 5, 5 n = 6

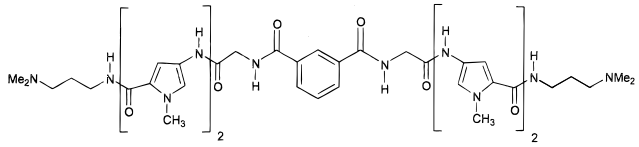

6

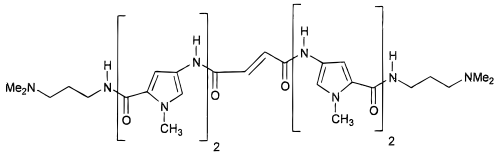

7

Hasselbach treatment of the ionization of weak acids and bases with the concept of the partition coefficient (*P*) between two immiscible solvents, giving eq 1, for a compound with one basic center:

$$D = P/(1 + 10^{(pK_a - pH)}) \qquad (1)$$

In this equation, *D* is defined as the ratio of the concentration of nonionized material in the organic (lipid) phase to the concentration of the combined ionized and nonionized material in the aqueous phase, at equilibrium. Since, for a given compound *P* and pK_a are constant, it is possible to plot log *D* against pH. Where insight is sought into the probable behavior of a molecule in the body, the region of greatest interest is that around pH 7.4, the pH of most body tissues. At pH 7.4 molecules such as **4**−**7** are expected to be doubly charged, in which case the pH-partition behavior is described by a special form of eq 1, taking account of the existence of two basic centers, here assumed to have the same value of pK_a, and a doubly charged species (eq 2). Where the two pK_a values are close, but not identical, this form of the equation can be regarded as an adequate approximation:

$$D = P/(1 + 2(10^{(pK_a - pH)}) + 10^{(2(pK_a - pH))}) \qquad (2)$$

Since the introduction of two charged groups might influence DNA binding, we compared the binding characteristics of compounds **4**−**7** using the footprinting technique.

Discussion

DNA Binding. We used DNase I and hydroxyl radical footprinting to examine the interaction of these ligands with natural and synthetic DNA fragments. With TyrT DNA (Figure 1), a natural DNA fragment which has been widely used in footprinting studies, we found that each of the compounds altered the digestion

TyrT DNA

5'-TCGGGAACCC$_{150}$CCACCACGGG$_{140}$GTATTGCTTT$_{130}$TTACTGGCCT$_{120}$GCT

CCCTTAT$_{110}$CGGGAAGCGG$_{100}$GGCGCATCAT$_{90}$ATCAAATGAC$_{80}$GCGCCGCT

GT$_{70}$AAAGTGTTAC$_{60}$GTTGAGAAAA$_{50}$AATGAACTGG$_{40}$TTGCGTAATT$_{30}$TTCA

TCCGTA$_{20}$ACGGATTAAA$_{10}$GGTAACCGGAA-3'

p(A/T)$_{6-12}$

5'-GATCCGGAATATTCCGGAAATATTTCCGGAAAATATTTTCCGGAAAAAT

ATTTTTCCGGATC-3'

pA$_{3-6}$

5'-GATCGCGTTTTTTCGCGTTTTTCGCGTTTTCGCGTTTCGCGATC-3'

p(A/T)$_{10}$

5'-GATCGCGTTTTTTAAAAACGCGTATATATATACGCGAAAAATTTTTCGCG

AATTCGCGATC-3'

p(A/T)$_6$

5'-GATCGCGAAATTTCGCGTATATACGCGTAATTACGCGTTTAAACGCGAA

TTCGCGG-3'

Figure 1. Sequences of the various DNA fragments used in this work. Only the strand bearing the radioactive label (underlined) is shown. TyrT is an *Eco*R1−*Ava*1 fragment. The numbering system used for this DNA is the same as that used in previous publications.[11−3] For p(A/T)$_{6-12}$, pA$_{3-6}$, p(A/T)$_{10}$, and p(A/T)$_6$ only the sequence of the insert (which was cloned into the *Bam*H1 site of pUC18) is shown. Every tenth base of the TyrT fragment is numbered for easy reference.

pattern at concentrations of 0.1−3 μM. In each case reductions in cleavage were seen around positions 25, 60, and 80, each of which corresponds to an AT-rich site which has previously been shown to be affected by other minor groove-binding ligands. These patterns were not easy to interpret since DNase I cleavage in the control was very uneven and several regions of poor cleavage in the control were located in the AT-rich regions around positions 25−30 and 45−50, which are expected to be good ligand-binding sites. We therefore repeated the experiments using hydroxyl radicals as the footprinting probe. These produced a much more even ladder of cleavage products in the control, enabling a more precise determination of the ligand-binding sites. Low concentrations of compound **4** (0.3 and 1 μM) produced attenuated cleavage around positions 25−30, 46−50, 61−65, and 81−86. The first two are located toward the 3′-side of long AT tracts (7 and 6 bases, respectively), while the third contains only 4 consecutive AT pairs. However, it may be significant that this lies within an AT-rich region; the 13 AT pairs between positions 59−71 contain only 3 GC pairs. It is possible that this represents ligand binding to a longer site (possibly TGTAAA at 65−70), tolerating a single guanine residue. Each of these footprints was about 6 bases long, compared with 3−4 bases observed with distamycin,[11] confirming the larger ligand-binding site. At higher concentrations (3 μM and above) the footprinting pattern changed and more regions were protected from cleavage. Most notable was a new footprint around position 40 (AACTGGTT). The regions protected around positions 60 and 80 also increased in size and appeared to split into two footprints located on either side of the ones produced at lower concentrations. The pattern produced by 1 μM **5** was similar to that generated by **4** at low concentrations, except that the footprint around position 65 was more clearly defined, while the footprint around position 25 extended over one or two more bases in the 3′-direction, consistent with its larger size. At higher concentrations (3 μM and above) hydroxyl radical cleavage was almost completely abolished. An example of a differential cleavage plot, derived from densitometer scans of the data for 1 μM compound **5** only, is presented in Figure 2A, revealing three distinct regions of protection between positions 20−70. Three clear footprints were also evident with 0.3 μM **7** around positions 25−30, 46−50, and 81−86, as observed with the other ligands, except that there was little protection around position 65. With 1 μM of ligand **7** new sites of protection were evident, corresponding to the pattern produced with higher concentrations of **4**. Compound **7** showed five binding sites between positions 20−77. The first and third (around positions 25 and 45) correspond to long AT tracts, while the latter (around position 65−70) contains the sequence TGTAAA. The other two sites are harder to define rigorously but appear to contain the sequences AACTGGTT (positions 37−44) and TTAGCTT (55−61). The changes with 1 μM **6** were less clear, with only one clear footprint at positions 27−31, with attenuated cleavage around positions 46−50 and 81−86.

These results confirm that the compounds are indeed AT-selective, with larger binding sites than the parent antibiotic distamycin. In addition they suggest that at moderate concentrations these compounds can bind to some sites which contain 1 or 2 GC base pairs and that the various derivatives have subtly different sequence binding properties. We have therefore investigated their interaction with several synthetic DNA fragments containing different length AT tracts and various arrangements of AT base pairs.

Fragment pAAD (not shown) contains 5 (A/T)$_4$ sites, each separated by 6 GC base pairs, and has previously been used to determine AT selectivity of several minor groove-binding ligands.[2] None of compounds **4**−**7** affected either DNase I or hydroxyl radical cleavage of this fragment at concentrations up to 3 μM, though higher concentrations abolished cleavage throughout the fragment. This confirms that, in this fragment, 4 consecutive AT base pairs were not sufficient to constitute a specific ligand-binding site.

Figure 3 shows DNase I cleavage of fragment pA$_{3-6}$ which contains 4 A$_n$/T$_n$ tracts of various lengths (n = 3−6). It can be seen that, with the exception of 3 μM **7**, cleavage of T$_3$ was not affected by the ligands and cleavage at T$_4$ was only attenuated at the highest ligand concentrations. Cleavage of T$_5$ and T$_6$ was inhibited at lower ligand concentrations with T$_6$ as the better site in each case. Both **4** and **7** protected T$_6$ at the lowest concentration (0.3 μM), while T$_5$ was not fully protected below 1 μM. Similarly **5** protected T$_6$ at 1 μM, while T$_5$ required 3 μM. For **6**, T$_6$ was protected at the highest concentration, while the other sites were hardly affected. It therefore appears that the ligands bind best to sites containing 6 consecutive AT base pairs, although there is a significant interaction with sites containing 5 and 4 AT pairs. Hydroxyl radical cleavage patterns with this fragment are not easy to interpret since digestion of the

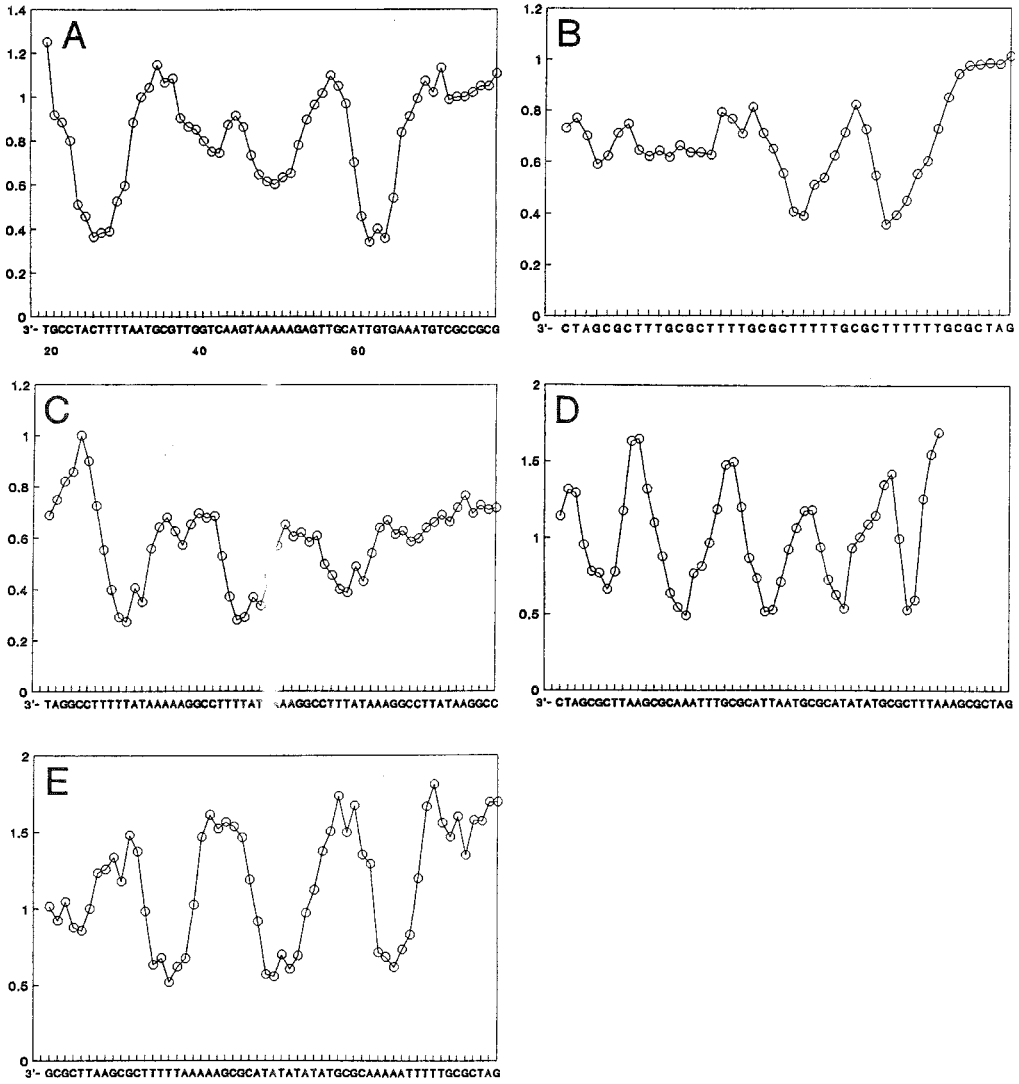

Figure 2. Differential cleavage plots showing the interaction of 1 μM **5** with the 5 different DNA fragments: A, TyrT DNA; B, pA_{3-6}; C, $p(A/T)_{6-12}$; D, $p(A/T)_6$; E, $p(A/T)_{10}$. The data were obtained from hydroxyl radical cleavage patterns and were analyzed as described in the text.

DNA was attenuated in each T_n tract in the absence of the ligand, consistent with previous suggestions that these sequences possess narrower than average minor grooves. A differential cleavage plot comparing the pattern in the presence of 1 μM **5** with that in the control is shown in Figure 2B. With this compound footprints were only produced at T_5 and T_6, each covering 6−7 bases. **6** also produced clear footprints at T_6 and T_5, and the protection at T_4 and T_3 coalesced into a single footprint. Compounds **4** and **7** produced footprints at all the T_n sites, each of which covers 5−6 bases. However, examination of the pattern at T_3 reveals that the apparent protection is far to the 3′-side of the actual site, suggesting that there was something unusual about this interaction.

The results with pA_{3-6} confirmed that the compounds bind best to longer AT tracts and showed that the binding site, as revealed by hydroxyl radicals, covered about 6 base pairs. We therefore extended these studies to a fragment containing longer AT tracts. With hydroxyl radical cleavage of $p(A/T)_{6-12}$, for which the sequence[13] is given in Figure 1, compounds **4** and **5** produced clear footprints covering 6−7 base pairs at the sites containing 8, 10, and 12 base pairs but had little effect on the upper site containing 6 AT base pairs (AATATT) (Figure 3). A differential cleavage plot showing the results for **5** is shown in Figure 2C. In contrast **7** produced footprints at all 4 sites, including AATATT. However the footprint at the longest site was much broader with this ligand affecting 8−9 base pairs. This may be because the ligand does not adopt a unique position within this long AT site but can assume one of several locations each of which does not cover the entire site. Surprisingly 1 μM **6** failed to show appreciable protection at any of the sites. It should be emphasized that each of these hydroxyl radical footprints is different from that produced by the parent antibiotic distamycin, which produces two distinct regions of protection within the 8-, 10-, and 12-base pair sites, consistent with the suggestion that two ligand molecules can simultaneously bind within each site.[13]

Previous studies have shown that, although distamycin and other minor groove-binding ligands can bind to all arrangements of 4 consecutive AT base pairs, some sites are better than others.[2] AATT is a particularly good binding site, while the ligands bind less well to

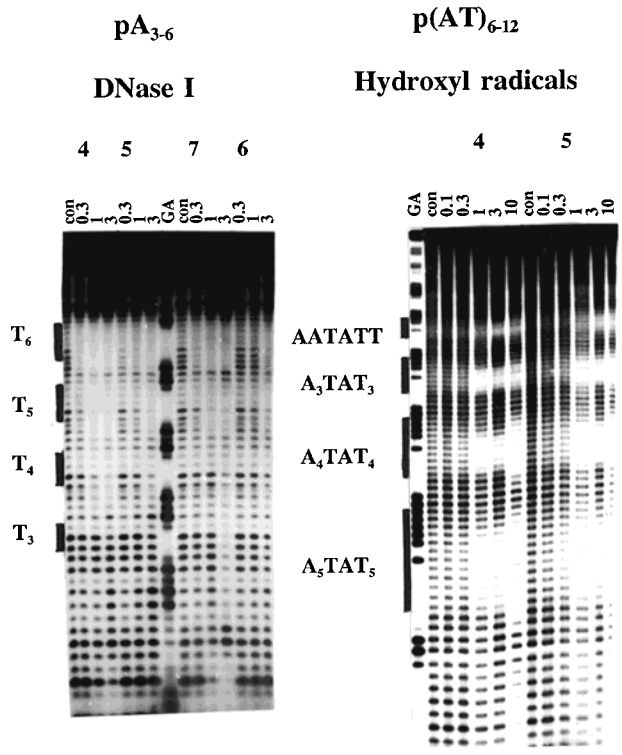

Figure 3. DNase I footprinting patterns for the interaction of compounds **4**−**7** with the fragments derived from pA_{3-6} and $p(AT)_{6-12}$. The concentration of the ligand (μM) is shown at the top of each gel lane. 'Con' indicates the control, in the absence of added ligand. Tracks labeled 'GA' are Maxam−Gilbert sequencing lanes specific for purines. The position of the various T_n blocks is indicated at the side of the autoradiograph.

sites containing TpA steps, especially TTAA and TATA. We therefore performed similar experiments with a fragment containing four different arrangements of 6 AT base pairs (A_3T_3, T_3A_3, $(TA)_3$, and TAATTA) together with AATT for comparison. The results of hydroxyl radical footprinting experiments with **5** on this fragment are shown in Figure 2D. Compounds **4**, **5**, and **7** produced DNase I footprints at each of the $(A/T)_6$ sites, while cleavage at AATT was not affected. The footprints at these various sites appeared at different ligand concentrations: cleavage at T_3A_3 and TAATTA was abolished at 0.2 μM **7**, while $(TA)_3$ required higher ligand concentrations (1 μM) to produce a footprint. No data could be obtained for A_3T_3 since this region showed no cleavage in the drug-free controls. The rank order of binding sites for these ligands is T_3A_3 > TAATTA > $(TA)_3$. It therefore appears that the binding strength decreases with increasing numbers of TpA steps. Compound **6** only affected enzyme cleavage at concentrations of 3 μM and above, though once again protection of $(TA)_3$ was weaker. A differential cleavage plot for hydroxyl radical cleavage of this fragment in the presence of 1 μM **5** is shown in Figure 2D. This confirms the binding sites and reveals that between 5−7 residues are protected at each position. Figure 2E shows a similar differential cleavage plot for hydroxyl radical cleavage of the fragment containing blocks of 10 AT base pairs in the presence of 1 μM **5**. These results are in contrast to those with distamycin,[13] which produces two distinct footprints at each AT site. This difference is consistent with the larger binding site size for these ligands, so that only one molecule is bound in each AT tract. Once again, between 5−7 bases are protected at each $(A/T)_{10}$ site, with much weaker binding at AATT. DNase I cleavage of this fragment shows protection at all the $(A/T)_{10}$ sites but reveals that the ligands do not discriminate between the different arrangements of AT base pairs.

Analogues **4** and **5** both have central regions which are simply extended polypyrroles. Above three pyrrole units, the hydrogen-bonding ability of the amide links ceases to be in-phase with the spacing on the floor of the minor groove,[6,14] resulting in a limit to the reading ability. The good affinity of these two analogues is therefore a reflection of the extra capacity for hydrophobic bonding in the minor groove. Their greater length, compared to the natural ligands, accounts for their preference for extended A/T base pair sequences. The glycine linkers in **6** are spaced appropriately for restoration of phasing with the H-bonding opportunities in the minor groove and were designed to be tolerant of, and perhaps selective toward, GC base pairs.[15] In this case, however, the hydrophilic nature of the amide links may affect binding to DNA and also would prejudice the chances of such a molecule reaching the site of action in vivo. Compound **6** is capable of weakly protecting short AT runs (not shown in the figures) which may indicate that the molecule is only binding at one end, with the central amide groups extending out into water, or that the molecule is behaving as a 'hairpin' and folding back to give side-by-side filling of the minor groove. To do this, at least one of the charges on the end amino groups would have to be lost by deprotonation.

Analogue **7** is a dimethylamino version of a head-to-head-linked netropsin analogue previously reported to display bidentate binding in $(AT)_n$-rich sequences.[16] This relatively rigid linker has a length of 4.2 Å, close to the 4.4 Å required to maintain the ideal phasing of ligand amide hydrogens. Although the central fumaramide unit has the right length, modeling indicates a distortion in the helicity of the molecule in the center, possibly accounting for the slightly weaker binding observed with this analogue.

Chemistry. For the construction of polypyrroles with a dimethylaminoalkyl end group, we used stepwise addition of *N*-methyl-4-nitro-2-trichloroacetylpyrrole units to amino-substituted mono- or polypyrroles with dimethylaminopropylamino tails (Scheme 1). The amino groups were generated by catalytic hydrogenation of the nitro group of the growing chain, an approach which was used to generate oligomers up to four rings in length. Addition of further rings resulted in a rapid decline in yield.

The syntheses of **4** and **5** were therefore based on the coupling of a two-ring and a three- or four-ring unit in a convergent fashion, in good yield (Scheme 1). This route was designed to allow a flexible approach to the synthesis of longer and more complex lexitropsins in the future. Analogue **4** was constructed by coupling a three-ring amine (Scheme 1) to a two-ring acid (Scheme 2), using HBTU/Et_3N, followed by HPLC purification. The hexapyrrole **5** followed similarly, from a four-ring amine and a two-ring acid.

Scheme 1[a]

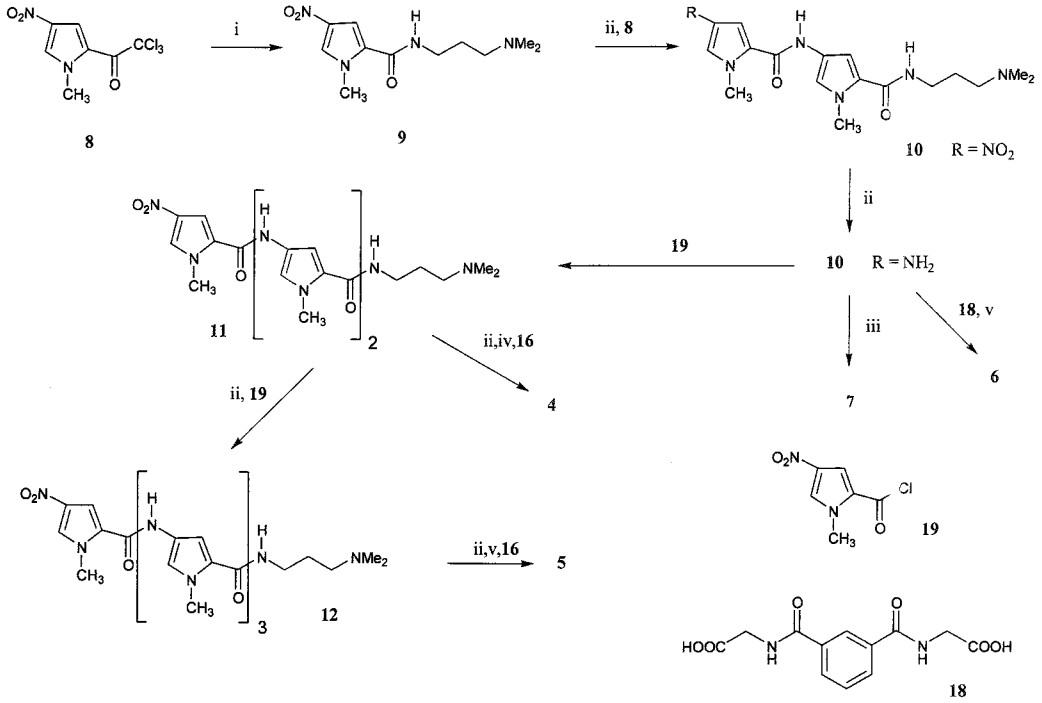

[a] Reagents: (i) $NH_2(CH_2)_3NMe_2$, rt; (ii) $Pd/C/H_2$; (iii) fumaric acid, HBTU, NMM; (iv) HBTU, Et_3N, DMF; (v) HBTU, NMM, DMF.

Scheme 2[a]

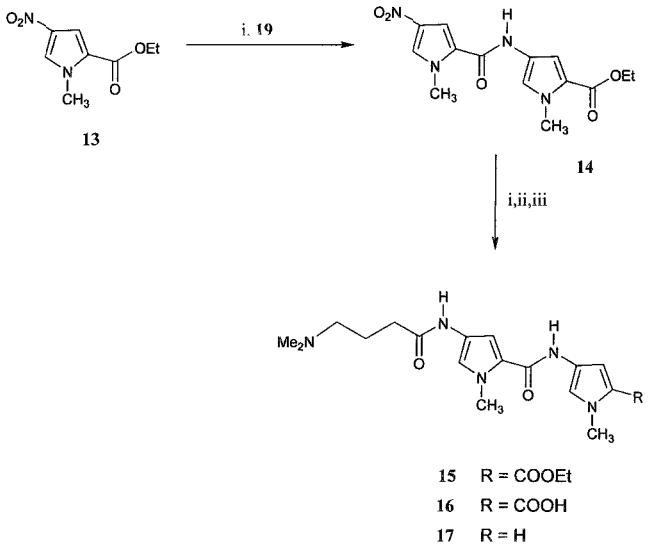

[a] Reagents: (i) $Pd/C/H_2$; (ii) $HOOC(CH_2)_3NMe_2$/HBTU/Et_3N/DMF; (iii) NaOH.

The isophthalic diamide **6** was synthesized in good yield, by first treating isophthaloyl chloride with glycine methyl ester to give **18**, followed by hydrolysis and coupling to **10** (R = NH_2), using HBTU/NMM (Scheme 1). Derivative **7** came directly from the coupling of the two-ring amine **10** (R = NH_2), used in the previous syntheses, with fumaric acid (Scheme 1).

Partitioning. Application of eq 1 to distamycin **(2)**, which has expected pK_a ca. 12.4 and calculated[17] log *P* value of −0.87, gives the curve shown in Figure 4, showing the effect of the very strongly basic amidine moiety, cf. acetamidine.[18] At pH 7.4, distamycin is expected to favor the aqueous phase, with potential difficulty in passing through a series of lipid membrane barriers. Calculated values of log *P*, assumed values of pK_a, and the resulting calculated values of log *D* at pH 7.4 for compounds **1**−**7** are given in Table 1.

Table 1. Input Data and Calculated log Distribution Coefficients for Extended Lexitropsins

compd	log P[a]	pK_a[b]	log D (pH 7.4)[c]
1	−3.29	12.4	−13.29
2	−0.87	12.4	−5.87
3	2.17	9.5	0.07
4	3.89	9.5	−0.32
5	4.68	9.5	0.47
6	1.47	9.5	−2.74
7	3.18	9.5	−1.03

[a] Calculated using the program in ref 17. [b] Assumed figures. [c] Calculated from eqs 1 and 2.

If the amidine is replaced with a dimethylaminoalkyl substituent, giving **3**, which has been found to be consistent with maintenance of DNA binding,[19] the pK_a is reduced by about 2 log units, by analogy with a range of compounds such as imipramine[20] and log *P* is increased by ca. 3 log units, giving the curve in Figure 4. Inspection of the curve shows that the behavior in the critical region about pH 7.4 is markedly affected: no longer is there such a strong preference for the aqueous phase. Such an analogue would be expected to show much improved bioavailability.

Relatively small molecules such as **1**−**3** would be expected to be sufficiently water-soluble to be capable of formulation as drugs. Longer DNA reading frames, however, require long stretches of hydrophobic bases, which by definition are likely to be less-water-soluble. Introduction of a second dimethylaminoalkyl group at the opposite end of the molecule to the first one, as in **4**−**7**, offers the possibility of improvement in water solubility.

The two basic centers are sufficiently far apart to behave as individual units, with the same or very

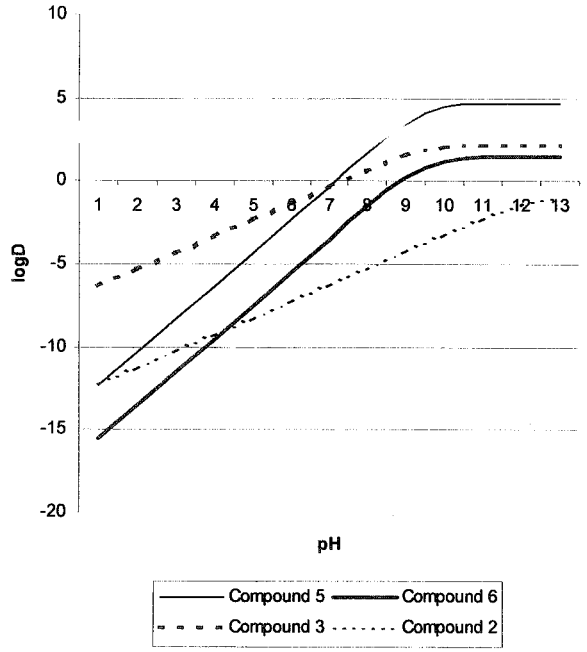

Figure 4. pH-partition behavior of compounds **2**, **3**, **5,** and **6** calculated from eqs 1 and 2.

similar pK_a values, which by analogy[20] we expect to be in the range 9−10. Figure 4 shows the pH-partition behavior of the most (**5**) and least (**6**) lipophilic of the dibasic analogues described in the present study, calculated from eq 2. Comparison of the data in Figure 4 shows the very marked effect of the second basic center, in **5** and **6**, in the region about pH 7.4. It is apparent that such analogues can tolerate much larger lipophilic 'loads' in the central region; of these analogues, the polypyrrole **5**, with the highest calculated value of log *P*, promises the kind of partitioning behavior consistent with good bioavailability. All of the dibasic compounds in the present study were readily water-soluble.

Overall, the significance of these results lies not only with the sequence-reading ability of these particular molecules but in the finding that water solubility can be a designed attribute, without compromising the physicochemical characteristics theoretically required for tissue penetration and maintaining affinity for DNA. It is becoming increasingly apparent, especially with the larger molecules required for extended sequence recognition in DNA, that drug design must take account of solubility and tissue penetration as primary features,[19] alongside receptor affinity and selectivity. In this context, the insertion of extra amide links to change hydrogen-bond phasing, as in **6**, must be approached with caution, since an amide makes a strong negative contribution to the log *P*. However, if attention is paid to the pH-partitioning characteristics of designed molecules, there is no reason lexitropsins cannot be designed to read long lengths of DNA and also have adequate bioavailability.

Experimental Section

Chemistry. ^{1}H NMR spectra were recorded at 400 MHz on a Bruker AMX spectrometer. Electrospray mass spectra were recorded on a Fisons VG Platform Benchtop LC−MS and EIMS on a JEOL JMS-AX505HA mass spectrometer. HPLC purifications were effected on a Vydac Protein and Peptide C18 column using a solvent gradient with two solvents: 0.1% TFA in water (A) and acetonitrile 90%, water 10%, TFA 0.1% (B). Elution commenced with 95% A, 5% B and finished with 100% B. Accurate mass measurements of compounds **4**−**7** were carried out at the EPSRC National Mass Spectrometry Service Centre, University of Wales, Swansea, U.K.

3-(1-Methyl-4-nitropyrrole-2-carboxamido)dimethylaminopropane, 9. A literature procedure[21] gave **9** in 90% yield: mp 130−131 °C (lit.[21] mp 129−130 °C).

3-[1-Methyl-4-(1-methyl-4-nitropyrrole-2-carboxamido)-pyrrole-2-carboxamido]dimethylaminopropane, 10. A literature procedure[21] gave **10** in 78% yield: mp 191−192 °C (lit.[21] mp 190−191 °C).

3-{1-Methyl-4-[1-methyl-4-(1-methyl-4-nitropyrrole-2-carboxamido)pyrrole-2-carboxamido]pyrrole-2-carboxamido}dimethylaminopropane, 11. A literature procedure[21] gave **11** in 63% yield: mp 198 °C (lit.[21] mp 136−137 °C; lit.[22,23] mp 205−206 °C).

(2*E*)-N^1,N^4-Bis[5-({[5-({[3-dimethylaminopropyl]amino}carbonyl)-1-methyl-1*H*-pyrrol-3-yl]amino}carbonyl)-1-methyl-1*H*-pyrrol-3-yl]-2-butenediamide Bistrifluoracetate, 7. 10, R = NO_2 (200 mg, 0.53 mmol), and Pd/C-10% (200 mg) were suspended in 2-propanol (25 mL) and hydrogenated for 4 h at room temperature. Filtration of the catalyst over Kieselguhr under N_2 followed by removal of the solvent in vacuo gave the amine **10**, R = NH_2, as an off-white solid that was used without further purification. Fumaric acid (25 mg, 0.22 mmol), HBTU (190 mg) and *N*-methylmorpholine (70 mL) were dissolved in DMF (1 mL, dry), with stirring at room temperature and then left for 30 min. The amine was dissolved in DMF (1.5 mL, dry) and added to the reaction mixture at room temperature with stirring. The reaction mixture was left stirring at room-temperature overnight, then purified by HPLC to give **7** as the bis-TFA salt (75 mg, 35% yield): ^{1}H NMR δ (DMSO-d_6) 1.24−1.84 (4H, p, 2CH_2), 2.79 (3H, s, NMe), 2.80 (3H, s, NMe), 3.05−3.10 (4H, m, 2CH_2), 3.24−3.27 (4H, m, 2CH_2), 3.82 (6H, s, 2NMe, pyrrole), 3.68 (6H, s, 2NMe, pyrrole), 6.93 and 6.94 (2H, d), 6.94 and 6.95 (2H, d), 7.09 (2H, s), 7.16 and 7.17 (2H, d), 8.13−8.16 (2H, t, 2CONH exchangeable), 9.32 (2H, broad 2TFA exchangeable), 9.92 (2H, s, 2CONH exchangeable), 10.47 (2H, s, 2CONH exchangeable); ES-MS found (M + 1) 773.4216, calcd for $C_{38}H_{53}N_{12}O_6$ 773.4211.

3-[1-Methyl-4-(1-methyl-4-(1-methyl-4-{1-methyl-4-nitropyrrole-2-carboxamido}pyrrole-2-carboxamido)pyrrole-2-carboxamido)pyrrole-2-carboxamido]dimethylaminopropane, 12. A mixture of **11** (1.00 g, 2.01 mmol) and Pd/C-10% (1.00 g) in ethanol (100 mL) was hydrogenated at room temperature for 20 h. The catalyst was removed by filtration through Kieselguhr and the filtrate evaporated under reduced pressure to give the crude amine as a pale yellow solid residue (772 mg, 82%). This amine (722 mg, 1.6502 mmol) was dissolved in dry DMF (3.0 mL) and the solution cooled in an ice bath and stirred while a solution of **8** (447 mg, 1.65 mmol) in dry DMF (1.0 mL) was added slowly during a period of 5 min. The resultant mixture was allowed to come to room temperature and stirred for 21 h. Water (30 mL) was added and the oily precipitate was scratched until it solidified. The solid was washed with water and, after drying in vacuo, amounted to 745 mg. Crystallization from aqueous methanol gave **12** (425 mg, 34% yield) as a yellow microcrystalline solid: mp 192−195 °C (lit.[24] mp 195 °C); ES-MS [M + 1] found 622.6, calcd for $C_{29}H_{36}N_{10}O_6$ 621.7; ^{1}H NMR (DMSO-d_6) δ 1.61 (2H, m, CH_2−*CH_2*−CH_2), 2.13 (6H, s, $N(CH_3)_2$), 2.24 (2H, t, CH_2−*CH_2*−NMe_2), 3.21 (2H, m, CONH−*CH_2*−CH_2), 3.80 (3H, s, NMe), 3.85 (3H, s, NMe), 3.87 (3H, s, NMe), 3.97 (3H, s, NMe), 6.83 (1H, d, ArH), 7.06 (2H, d, 2ArH), 7.19 (1H, d, ArH), 7.26 (1H, d, ArH), 7.29 (1H, d, ArH), 7.60 (1H, d, ArH), 8.09 (1H, t, CO-*NH*-CH_2, exchangeable), 8.20 (1H, d, ArH), 9.91 (1H, s, *CONH*, exchangeable), 10.01 (1H, s, *CONH*, exchangeable), 10.31 (1H, s, *CONH*, exchangeable).

Ethyl 1-Methyl-4-(1-methyl-4-nitropyrrole-2-carboxamido)pyrrole-2-carboxylate, 14. The nitro compound **13** (2.057 g, 10.39 mmol) was hydrogenated over 10% Pd/C (805 mg) in ethanol (200 mL) at room temperature for 2 h. The catalyst was removed by filtration through Kieselguhr and the

filtrate evaporated under reduced pressure to leave the crude amine as a gray oil. This oil was dissolved in an ice−water bath, while a solution of **19** (10.39 mmol, prepared[24] from 1.766 g of the carboxylic acid, using 2.0 mL of thionyl chloride, and 8 mL of DME) in dry DME (10 mL) was added slowly over a period of 5 min. The resultant mixture was stirred and allowed to come to room temperature overnight then it was evaporated under reduced pressure. The residue was stirred for 1 h with N HCl (50 mL) and the solid filtered, washed well with ethanol and dried in vacuo to give **14** as a yellow powder (1.377 g, 41% yield): mp 232−234 °C (lit.[26] mp 239−240 °C); IR (KBr) ν_{max} 3358, 3131, 1692, 1663, 1572, 1437, 1391, 1317, 1253, 1121 cm^{-1}; ^1H NMR (DMSO-d_6) δ 1.24−1.30 (3H, t, CH_2CH_3), 3.84 (3H, s, NMe), 3.94 (3H, s, NMe), 4.16−4.24 (2H, q, CH_2CH_3), 6.90−6.91 (1H, d), 7.42−7.43 (1H, d), 7.54−7.55 (1H, d), 8.18−8.19 (1H, d), 10.26 (1H, s, *CONH* exchangeable).

Ethyl 1-Methyl-4-(1-methyl-4-(4-dimethylaminobutyryl)-amino)pyrrole-2-carboxylate, 15. A mixture of **14** (605 mg) and Pd/C-10% (627 mg) in ethanol (60 mL) was hydrogenated at room temperature for 16 h. The catalyst was removed by filtration through Kieselguhr and the filtrate was evaporated under reduced pressure to leave the crude amine as a buff colored glassy foam (456 mg, 83% yield) which was used without further purification. A mixture of 4-dimethylamino-butyric acid hydrochloride (527 mg, 3.15 mmol, 2 equiv), HBTU (1.1923 g, 3.15 mmol, 2 equiv), Et_3N (1.31 mL, 6 equiv) and dry DMF (7.0 mL) was placed under N_2 and stirred at room temperature for 30 min. Then to the stirred mixture was slowly added a solution of the above amine (456 mg, 1.57 mmol, 1 equiv) in dry DMF (2.5 mL) over a period of 5 min. After stirring at room temperature for 3 h the resultant mixture was diluted with EtOAc (250 mL) then extracted with 10% Na_2CO_3 (100 mL). The organic layer was washed with brine, dried ($MgSO_4$), and evaporated under reduced pressure to leave a red-brown oil (1.036 g). The crude product was purified by flash column chromatography over silica, using MeOH containing 3% of concentrated ammonia as eluant, to give **15** as an amber oil (487 mg, 77% yield): ES-MS [M + 1] found 404.2, calcd for $C_{20}H_{29}N_5O_4$ 404.5; ^1H NMR (DMSO-d_6) δ 1.24 (3H, t, O−CH_2−CH_3), 1.66 (2H, m, CH_2−CH_2−CH_2), 2.08 (6H, s, NMe_2), 2.20 (4H, m, CH_2−CH_2−CH_2), 3.77 (3H, s, pyrrole NMe), 3.79 (3H, s, pyrrole NMe), 4.17 (2H, q, O−CH_2−CH_3), 6.80 (1H, d, ArH), 7.12 (1H, d, ArH), 7.36 (1H, d, ArH), 9.80 (1H, s, CONH, exchangeable), 9.90 (1H, s, CONH, exchangeable).

1-Methyl-4-(1-methyl-4-(4-dimethylaminobutyryl)amino)pyrrole-2-carboxamido)pyrrole-2-carboxylic Acid, 16. A solution of **15** (465 mg, 1.15 mmol) in EtOH (5 mL) and NaOH (1.73 mmol) was heated under reflux for 1 h and then concentrated under reduced pressure. The residue was dissolved in MeOH (5 mL) containing 3% of concentrated NH_4-OH, and the resultant solution was applied to a flash column of silica. The column was eluted first with a mixture of EtOAc (60 parts) and MeOH containing 3% concentrated NH_4OH (40 parts), to elute any unreacted ester **15** and any decarboxylation product **17**, then MeOH containing 3% of concentrated NH_4-OH was used to elute the carboxylic acid **16**. After evaporation water was removed from the residue by coevaporation with EtOH, and finally the residue was triturated with Et_2O until it solidified. After drying in vacuo the product was obtained as a cream-colored powder (258 mg, 60% yield): mp 138 °C (gas evolution); ES-MS [M + 1] found 376.2, calcd for $C_{18}H_{25}N_5O_4$ 376.4; IR (KBr) ν_{max} 1639, 1617, 1566 cm^{-1}; ^1H NMR (DMSO-d_6) δ 1.69 (2H, m, CH_2−CH_2−CH_2), 2.14 (6H, s, NMe_2), 2.26 (4H, m, CH_2−CH_2−CH_2; after the addition of D_2O this became 2H, t, and a new triplet for 2H appeared at 2.85), 3.81 (6H, s, 2 × pyrrole NMe), 6.78 (1H, d, ArH), 6.85 (1H, d, ArH), 7.15 (1H, d, ArH), 7.37 (1H, d, ArH), 9.82 (1H, s, exchangeable, CONH), 9.83 (1H, s, exchangeable, CONH). The CO_2H signal was not observed.

Note: It was inadvisable to acidify the product of this hydrolysis. Whenever this was done, either by using HCl, or by attempting to isolate the product by reverse-phase HPLC using an acidic (TFA) solvent system, considerable decarboxylation occurred to give **17**. This decarboxylation product had a very close HPLC retention time to that of **16**, but separation could be accomplished using flash column chromatography over silica using EtOAc/MeOH/NH_4OH as eluant as described above. Compound **17** was thus isolated from one experiment as an amber gum: ES-MS 332.1, calcd for $C_{17}H_{25}N_5O_2$ 332.4 [M + 1]; ^1H NMR (DMSO-d_6) δ 1.79 (2H, m, CH_2−CH_2−CH_2), 2.28 (2H, m, CH_2), 2.34 (6H, s, NMe_2), 3.38 (2H, m, CH_2), 3.55 (3H, s, pyrrole NMe) 3.80 (3H, s, pyrrole NMe), 6.05 (1H, m, ArH), 6.52 (1H, m, ArH), 6.81 (1H, d, ArH), 7.08 (1H, m, ArH), 7.13 (1H, d, ArH), 9.71 (1H, s, exchangeable, CONH), 9.86 (1H, s, exchangeable, CONH).

3-(1-Methyl-4-(1-methyl-4-(1-methyl-4-(1-methyl-4-(1-methyl-4-(4-dimethylaminobutyryl)aminopyrrole-2-carboxamido)pyrrole-2-carboxamido)pyrrole-2-carboxamido)pyrrole-2-carboxamido)pyrrole-2-carboxamido)dimethylaminopropane Bistrifluoracetate, 4. A mixture of **11** (151 mg) and Pd/C-10% (164 mg) in EtOH (15 mL) was hydrogenated at room temperature for 13 h. The catalyst was removed by filtration through Kieselguhr, and the filtrate evaporated under reduced pressure to leave the crude amine (128.5 mg, 90% yield) as a pale yellow solid. This material was used at once without further purification. A mixture of the carboxylic acid **16** (68.6 mg, 0.18 mmol, 1 equiv), HBTU (104.1 mg, 0.275 mmol, 1.5 equiv), Et_3N (76 mL, 55.5 mg, 0.55 mmol, 3 equiv) and dry DMF (1.5 mL) was placed under N_2 and stirred at room temperature for 30 min. To the resultant clear solution was added a solution of the above crude amine (128.5 mg, 0.275 mmol, 1.5 equiv) in dry DMF (1.0 mL), and the mixture stirred at room temperature for 8 h. The resultant suspension was purified by reverse-phase HPLC. Fractions containing the product were frozen immediately after collection and then freeze-dried to give the bis-TFA salt **4** as a fawn powder (65.3 mg, 34% yield): ES-MS found [M + 1] 826.4476, calcd for $C_{41}H_{56}N_{13}O_6$ 826.4476; ^1H NMR (DMSO-d_6) δ 1.82−1.93 (4H, 2 × overlapping quintets, 2 × CH_2−CH_2−CH_2), 2.35 (2H, t, CH_2−CH_2−CO), 2.79 (12H, m, 2 × NMe_2), 3.07 (4H, m, 2 × CH_2−CH_2−NMe_2), 3.24 (2H, m, NH−CH_2−CH_2), 3.72−3.86 (15H, 5 × pyrrole NMe), 6.87−7.22 (10H, 10 × ArH), 8.14 (1H, t, exchangeable *CONH*−CH_2), 9.2−9.5 (2H, broad, exchangeable, 2 × TFA), 9.89−9.94 (5H, exchangeable, 5 × CONH).

3-(1-Methyl-4-(1-methyl-4-(1-methyl-4-(1-methyl-4-(1-methyl-4-(1-methyl-4-(4-dimethylaminobutyryl)amino-pyrrole-2-carboxamido)pyrrole-2-carboxamido)pyrrole-2-carboxamido)pyrrole-2-carboxamido)pyrrole-2-carboxamido)pyrrole-2-carboxamido)dimethylaminopropane Bistrifluoracetate, 5. The nitro compound **12** (1125 mg) was hydrogenated in a mixture of MeOH (10.5 mL) and 0.1 N HCl (4.5 mL) over Pd/C-10% (125 mg) as described in the previous experiment above, to afford, after freeze-drying, the crude amine (112.5 mg, 84%). This amine was mixed with the carboxylic acid **16** (42.4 mg, 0.11 mmol), HBTU (64.2 mg, 0.17 mmol), NMM (50 mL) and DMF(1.0 mL, dry), and the resultant mixture was stirred at room temperature for 24 h. The product was isolated by means of reverse-phase HPLC. Fractions containing the product were frozen immediately on collection then freeze-dried to give the bis-TFA salt of **5** as a buff-colored powder (58.3 mg, 37% yield) which had no distinct melting point: ES-MS found [M + 1] 948.4964, calcd for $C_{47}H_{62}N_{15}O_7$ 948.4956; ^1H NMR (DMSO-d_6) δ 1.82−1.93 (4H, 2 × overlapping quintets, 2 × CH_2−CH_2−CH_2), 2.35 (2H, t, CH_2-CH_2−CO), 2.79 (12H, m, 2 × NMe_2), 3.07 (4H, m, 2 × CH_2−CH_2−NMe_2), 3.24 (2H, m, NH−CH_2−CH_2), 3.82−3.87 (18H, 6 × pyrrole NMe), 6.87−7.22 (12H, 12 × ArH), 8.15 (1H, t, exchangeable, *CONH*−CH_2), 9.30 (1H, broad, exchangeable, TFA), 9.50 (1H, broad, exchangeable, TFA), 9.90−9.94 (6H, exchangeable, 6 × *CONH*).

Isophthalamidodiacetic Acid, 18. A stirred suspension of isophthaloyl chloride (200 mg, 1.00 mmol) and glycine methyl ester hydrochloride (275 mg, 2.20 mmol) in anhydrous methylene chloride (20 mL) was treated dropwise with a solution of triethylamine (0.66 g, 6.60 mmol) in dry methylene chloride (5 mL). The resulting solution was then stirred at

room temperature for 1.5 h. The solvent was evaporated and the residue treated with 2 M HCl (5 mL) then extracted with methylene chloride. Evaporation of the extract gave the required product as a pale yellow gum (210 mg, 75% yield): ^{1}H NMR (DMSO-d_6) δ 3.66 (6H, s, 2 × OMe), 4.04 (4H, d, J 6 Hz, 2 × NHCH_2, collapses to a singlet on addition of D_2O), 7.62 (1H, t, J 8 Hz, ArH), 8.03 (2H, dd, J_o 8 Hz, J_m 2 Hz, 2 × ArH), 8.38 (1H, m, ArH), 9.12 (2H, t, J 6 Hz, *COHN*); EI-MS found 308.1026, calcd for $C_{14}H_{16}N_2O_6$ 308.2220. A solution of the dimethyl ester (690 mg, 2.30 mmol) in ethanol (30 mL) was treated with 2 M NaOH (15 mL) and the resulting solution stirred at room temperature for 1 h. The mixture was concentrated by evaporation to a total volume of 10−15 mL then acidified with 2 M HCl and extracted with ethyl acetate. Evaporation of the extract gave **18** as a colorless solid (260 mg, 41% yield): mp 152−154 °C; ^{1}H NMR (DMSO-d_6) δ 3.94 (4H, d, J 6 Hz, CH_2 collapses to a singlet on addition of D_2O), 7.62 (1H, d, J 8 Hz, ArH), 8.03 (2H, dd, J_o 8 Hz, Jm 2 Hz, 2 × ArH), 8.37 (1H, s, ArH), 8.98 (2H, t, J 6 Hz, 2 × *CONH*CH_2 exchangeable), 13.12 (2H, broad, CO_2H exchangeable); ES-MS found 279.01 [M − 1], calcd for $C_{12}H_{12}N_2O_6$ [M − 1] 279.17.

***N*¹,*N*³-Bis(2-{[5-({[5-({[3-dimethylaminopropyl]amino}carbonyl)-1-methyl-1*H*-pyrrol-3-yl]amino}carbonyl)-1-methyl-1*H*-pyrrol-3-yl]amino}-2-oxoethyl)isophthalamide Bistrifluoracetate, 6.** A solution of the dicarboxylic acid **18** (28 mg, 0.1 mmol), NMM (30 mg, 0.3 mmol) and HBTU (165 mg, 0.3 mmol) in DMF (1 mL, dry) was stirred at room temperature for 1 h. The mixture was then treated with a solution of freshly prepared **10**, R = NH_2 [prepared beforehand by hydrogenating a suspension of **10**, R = NO_2 (165 mg, 0.3 mmol) with Pd/C-10% (165 mg) in 2-propanol (20 mL) for 6 h] in dry DMF (1 mL). The resulting solution was stirred at room temperature overnight. The mixture was then purified by HPLC to give the required product (60 mg, 52% yield) as a pale yellow solid (bis-TFA salt) with no distinct melting point: ^{1}H NMR (DMSO-d_6) δ 1.83 (4H, m, J 7 Hz, CH_2CH_2-CH_2), 2.78 (12H, d, J 4 Hz, 4 × NHMe_2), 3.07 (4H, m, CONHCH_2, collapses to a triplet on addition of D_2O), 3.24 (4H, m, 2 × Me_2NHCH_2, collapses to a triplet on addition of D_2O), 3.81 (6H, s, 2 × NMe), 3.83 (6H, s, 2 × NMe), 4.04 (4H, d, J 6 Hz, NHCH_2CO, collapses to a singlet on addition of D_2O), 6.91−6.93 (4H, m, 2 × ArH), 7.15 (2H, d, J 2 Hz, ArH), 7.17 (2H, d, J 2 Hz, ArH), 7.61 (1H, t, J_o 8 Hz, ArH), 8.06 (2H, dd, J_o 8 Hz, J_m 2 Hz, ArH), 8.14 (2H, t, J 6 Hz, 2 × *NH*CH_2, exchangeable), 8.43 (1H, s, ArH), 8.91 (2H, t, J 6 Hz, 2 × *CONH*, exchangeable), 9.27 (2H, broad, 2 × *NH*Me_2, exchangeable), 9.85 (2H, s, 2 × *CONH*, exchangeable), 9.96 (2H, s, 2 × *CONH*, exchangeable); ES-MS found [M + 1] 937.4804, calcd for $C_{46}H_{61}N_{14}O_8$ 937.4797.

Footprinting Studies. Ligands: The ligands were dissolved in 10 mM Tris-HCl pH 7.5 containing 10 mM NaCl at a concentration of 10 mM and stored at −20 °C. The compounds were diluted to working concentrations in the same buffer immediately before use. Oligonucleotides for preparing the DNA fragments containing synthetic DNA inserts were purchased from Oswel. DNase I was purchased from Sigma and stored at −20 °C at a concentration of 7200 units/mL.

DNA fragments: The sequences of the five most significant DNA fragments used in this work are shown in Figure 1. The TyrT fragment, derived[25] from plasmid pKMΔ-98, was obtained by digesting the plasmid with *Eco*R1 and *Ava*1 and labeled at the 3′-end of the *Eco*R1 site with [α-^{32}P]dATP using reverse transcriptase. Plasmid pAAD1 was prepared as previously described.[2] The other plasmids were prepared by cloning oligonucleotides into the *Sma*I site of pUC18 as previously described. pAAD1[2] contains an insert which possesses 5 different $(A/T)_4$ tracts, separated by 6 GC base pairs (CGCGCG). Plasmid pA_{3-6} contains 4 $T_n \times A_n$ tracts of varying length (n = 3−6) separated by 4 GC base pairs (CGCG). $p(A/T)_{6-12}$ contains 4 AT tracts of 6, 8, 10, and 12 bases long with the sequence A_nTAT_n (n = 2−5) separated by 4 GC base pairs (CCGG). Plasmid $p(AT)_6$ contains 4 different arrangements of $(A/T)_6$ sites together with the sequence AATT, each separated by 4 GC base pairs (CGCG). Plasmid $p(A/T)_{10}$ contains 3 different arrangements of $(A/T)_{10}$ sites together with the sequence AATT, each separated by 4 GC base pairs (CGCG). Polylinker DNA fragments containing each of these synthetic sequences were obtained by digesting with *Hin*dIII, labeling with [α-^{32}P]dATP using reverse transcriptase and digesting again with either *Eco*R1 ($p(A/T)_{6-12}$ and pA_{3-6}) or *Sac*1 ($p(A/T)_{10}$ and pAAD1). The labeled DNAs of interest were separated from the remainder of the plasmid on 6−8% polyacrylamide gels and dissolved in 10 mM Tris-HCl pH 7.5 containing 0.1 mM EDTA.

DNase I footprinting: Radiolabeled DNA (1.5 μL) was mixed with 1.5 μL of ligand (dissolved in 10 mM Tris-HCl pH 7.5 containing 10 mM NaCl) and left to equilibrate at room temperature for at least 30 min. 2 μL of DNase I (approximately 0.01 units/mL diluted in 20 mM NaCl containing 2 mM $MgCl_2$ and 2 mM $MnCl_2$) was then added. The reaction was stopped after 1 min by adding 4 μL of formamide containing 10 mM EDTA and 0.1% (w/v) bromophenol blue.

Hydroxyl radical footprinting: Radiolabeled DNA (2 μL) was mixed with 2 μL of ligand (dissolved in 10 mM Tris-HCl pH 7.5 containing 10 mM NaCl) and left to equilibrate at room temperature for at least 30 min. Digestion was initiated by adding 6 μL of a freshly prepared solution containing 30 μM ferrous ammonium sulfate, 300 μM EDTA, 3 mM ascorbic acid and 0.1% H_2O_2. The reaction was stopped after 10 min by adding 8 μL of 0.75 M sodium acetate and 60 μL of ethanol. The DNA was precipitated, washed with 70% ethanol, dried and redissolved in 8 mL of formamide containing 10 mM EDTA and 0.1% (w/v) bromophenol blue.

Gel electrophoresis: Samples were denatured by boiling for 3 min, cooled on ice and loaded onto denaturing polyacrylamide gels (6−10% w/v) containing 8 M urea. Gels (40 cm long) were run at 1500 V for about 2 h before fixing in 10% acetic acid (v/v), transferring to Whatman 3MM paper, drying under vacuum at 80 °C and exposing to autoradiography at −70 °C with an intensifying screen. Autoradiographs were scanned with a Hoefer 365W scanning microdensitometer. The intensity of each band was estimated using the Hoefer software. Differential cleavage plots, calculated from these scans, represent the intensity of each band in the drug-treated lane divided by the intensity of the corresponding band in the drug-free control.

References

(1) Wartel, R. M.; Larson, R. M.; Wells, R. D. A specific probe for A−T regions of duplex deoxyribonucleic acid. *J. Biol. Chem.* **1974**, *249*, 6719−6731.

(2) Abu-Daya, A.; Brown, P. M.; Fox, K. R. DNA sequence preferences of several AT-selective minor groove binding ligands. *Nucleic Acids Res.* **1995**, *23*, 3385−3392.

(3) Hamdan, I. I.; Skellern, G. G.; Waigh, R. D. Ligand binding to oligonucleotides. *Methods Mol Biol.*, in press.

(4) For example: Rao, K. E.; Shea, R. G.; Bathini, Y.; Lown, J. W. Molecular recognition between oligopeptides and nucleic acids − DNA-sequence specificity and binding properties of thiazole-lexitropsins incorporating the concepts of base site acceptance and avoidance. *Anti-Cancer Drug Des.* **1990**, *5*, 3−20. Dwyer, T. J.; Geierstanger, B. H.; Bathini, Y.; Lown, J. W.; Wemmer, D. E. Design and binding of a distamycin-A analogue to d(CGCAAGTTGGC)·d(GCCAACTTGCG) − synthesis, NMR studies and implications for the design of sequence-specific minor groove binding oligopeptides. *J. Am. Chem. Soc.* **1992**, *114*, 5912−5919. Geierstanger, B. H.; Mrksich, M.; Dervan, P. B.; Wemmer, D. E. Design of a G. C specific DNA minor-groove binder. *Science* **1994**, *266*, 646−650.

(5) Turner, J. M.; Baird, E. E.; Dervan, P. B. Recognition of seven base pair sequences in the minor groove of DNA by ten-ring pyrrole-imidazole polyamide hairpins. *J. Am. Chem. Soc.* **1997**, *119*, 7636−7644.

(6) For example: Guo, D.; Gupta, R.; Lown, J. W. DNA sequence-selective binding of head-to-tail linked bis-lexitropsins − relation of phasing to cytotoxic potency. *Anti-Cancer Drug Des.* **1993**, *8*, 369−397.

(7) Trauger, J. W.; Baird, E. E.; Dervan, P. B. Recognition of DNA by designed ligands at subnanomolar concentrations. *Nature* **1996**, *382*, 559−561. Herman, D. M.; Baird E. E.; Dervan, P. B. Stereochemical control of the DNA binding affinity, sequence specificity and orientation preference of chiral hairpin polyamides in the minor groove. *J. Am. Chem. Soc.* **1998**, *120*, 1382−1391.

(8) Haq, I.; Ladbury, J. E.; Chowdrhy, B. Z.; Jenkins, T. C.; Chaires, J. B. Specific binding of Hoechst 33258 to the $(CGCAAATTTGCG)_2$ duplex: calorimetric and spectroscopic studies. *J. Mol. Biol.* **1997**, *271*, 244−257.
(9) For example: Singh, M. P.; Plouvier, B.; Hill, G. C.; Gueck, J.; Pon, R. T.; Lown, J. W. Isohelicity and strand selectivity in the minor groove binding of chiral (1R,2R)-bis(netropsin)-1,2-cyclopropanedicarboxamide and (1S,2S)-bis(netropsin)-1,2-cyclopropanecarboxamide ligands to duplex DNA. *J. Am. Chem. Soc.* **1994**, *116*, 7006−7020. Wang, A. H. J.; Cottens, S.; Dervan, P. B.; Yesinowski, J. P.; Vandermarel, G. A.; Vanboom, J. H. Interactions between a symmetrical minor groove binding compound and DNA oligonucleotides − H-1 and F-19 NMR studies. *J. Biomol. Struct. Dyn.* **1989**, *7*, 101−117.
(10) Florence, A. T.; Attwood, D. *Physicochemical Principles of Pharmacy*, 3rd ed.; Macmillan: London, 1998; p 185.
(11) Fox, K. R.; Waring, M. J. DNA structural variations produced by actinomycin and distamycin as revealed by DNAase I footprinting. *Nucleic Acids Res.* **1984**, *12*, 9271−9285.
(12) Portugal, J.; Waring, M. J. Hydroxyl radical footprinting of the sequence-selective binding of netropsin and distamycin to DNA. *FEBS Lett.* **1987**, *225*, 195−200.
(13) Abu-Daya, A.; Fox, K. R. Interaction of minor groove binding ligands with long AT-tracts. *Nucleic Acids Res.* **1997**, *25*, 4962−4969 and unpublished observations.
(14) Lown, J. W. Lexitropsins − rational design of DNA-sequence reading agents as novel anti-cancer agents and potential cellular probes. *Anti-Cancer Drug Des.* **1988**, *3*, 25−40.
(15) Waszkowycz, B. Unpublished data.
(16) Rao, K. F.; Zimmerman, J.; Lown, J. W. Sequence-selective DNA-binding by linked bis-*N*-methylpyrrole dipeptides − an analysis by MPE footprinting and force-field calculations. *J. Org. Chem.* **1991**, *56*, 786−797.
(17) Leo, A. The octanol−water partition coefficient of aromatic solutes − the effect of electronic interactions, alkyl chains, hydrogen bonds and ortho-substitution. *J. Chem. Soc., Perkin Trans. 2* **1983**, 825−838 and references cited therein.
(18) Sykes, P. *A Guidebook to Mechanism in Organic Chemistry*, 4th ed.; Longman: London, 1975; p 68.
(19) Zhao, R.; Lown, J. W. Synthesis of a novel N-methoxymethylpyrrole-containing DNA minor-groove binding oligopeptide related to distamycin. *Heterocycles* **1995**, *41*, 337−344.
(20) Green, A. L. Ionization constants and water solubilities of some aminoalkylphenothiazine tranquillizers and related compounds. *J. Pharm. Pharmacol.* **1967**, *19*, 10−16.
(21) Nishiwaki, E.; Tanaka, S.; Lee, H.; Shibuya, M. Efficient synthesis of oligo-*N*-methylpyrrolecarboxamides and related compounds. *Heterocycles* **1988**, *27*, 1945−1952.
(22) Glibin, E. N.; Tsukerman, B. V.; Ginzburg, O. F. Analogue of distamycin A with a dimethylamino group. *J. Org. Chem. USSR (Engl. Transl.)* **1977**, *13*, 2082−2083.
(23) Glibin, E. N.; Tsukerman, B. V.; Ginzburg, O. F. Synthesis of actinomycin analogues. X. Polyfunctional DNA complexing agents. *J. Org. Chem. USSR (Engl. Transl.)* **1981**, *17*, 568−572.
(24) Arcamone, F.; Nerviano, M.; Mongelli, N.; Penco, S. Poly-4-aminopyrrole-2-carboxamide derivatives, procedures for their preparation, and antiviral and antineoplastic pharmaceuticals containing them. Ger. Offen. DE 3,623,880, Jan 29, 1987.
(25) Drew, H. R.; Travers, A. A. DNA structural variations in the *E. coli tyr*T promoter. *Cell* **1984**, *37*, 491−502.
(26) Turchin, K. F.; Grokhovskii, S. L.; Zhuze, A. L.; Gottikh, B. P. Ligands possessing affinity for definite pairs of DNA bases. II. A study of the stereochemistry of the chromophore of distamycin A by ^{1}H NMR spectroscopy. *Sov. J. Bioorg. Chem.* (*Engl. Transl.*) **1978**, *4*, 780−790.

JM990620E